

Specification of vertebral identity is coupled to Notch signalling and the segmentation clock

Ralf Cordes, Karin Schuster-Gossler, Katrin Serth and Achim Gossler*

Institut für Molekularbiologie OE5250, Medizinische Hochschule, Carl-Neuberg-Str. 1, D-30625 Hannover, Germany

*Author for correspondence (e-mail: gossler.achim@mh-hannover.de)

Accepted 10 December 2003

Development 131, 1221–1233

Published by The Company of Biologists 2004

doi:10.1242/dev.01030

Summary

To further analyse requirements for Notch signalling in patterning the paraxial mesoderm, we generated transgenic mice that express in the paraxial mesoderm a dominant-negative version of Delta1. Transgenic mice with reduced Notch activity in the presomitic mesoderm as indicated by loss of *Hes5* expression were viable and displayed defects in somites and vertebrae consistent with known roles of Notch signalling in somite compartmentalisation. In addition, these mice showed with variable expressivity and penetrance alterations of vertebral identities resembling homeotic transformations, and subtle changes of Hox gene expression in day 12.5 embryos. Mice that carried only one functional copy of the endogenous *Delta1* gene also showed changes of vertebral identities in the lower cervical region, suggesting a

previously unnoticed haploinsufficiency for Delta1. Likewise, in mice carrying a null allele of the oscillating *Lfng* gene, or in transgenic mice expressing *Lfng* constitutively in the presomitic mesoderm, vertebral identities were changed and numbers of segments in the cervical and thoracic regions were reduced, suggesting anterior shifts of axial identity. Together, these results provide genetic evidence that precisely regulated levels of Notch activity as well as cyclic *Lfng* activity are critical for positional specification of the anteroposterior body axis in the paraxial mesoderm.

Key words: Notch signalling, Vertebral identity, Somitogenesis, Positional specification, Mouse

Introduction

The vertebral column is a segmented structure characteristic for all vertebrates. The segmental pattern is established early during embryogenesis by the generation of somites. In most vertebrate species somites are blocks of epithelial cells that condense sequentially from the paraxial mesoderm on both sides of the neural tube in a strict anterior to posterior order. In mouse embryos, the first somites form in the posterior head-fold region at approximately day 7.75 of development. During the subsequent five days somite condensation progresses, while concomitantly new mesoderm cells are being generated caudally from the primitive streak and later from the tail bud elongating the embryo posteriorly (Gossler and Tam, 2002).

Somite formation and patterning require cell-to-cell communication in the presomitic mesoderm (psm) mediated by the Notch signalling pathway. Mutations in genes encoding Notch pathway components in mouse disrupt compartmentalization of somites, and alignment and maintenance of segment borders (Conlon et al., 1995; del Barco Barrantes et al., 1999; Evrard et al., 1998; Hrabé de Angelis et al., 1997; Kusumi et al., 1998; Swiatek et al., 1994; Zhang and Gridley, 1998). Somite formation involves a molecular oscillator termed the ‘segmentation clock’ that operates in the presomitic mesoderm and manifests itself by the periodic expression of ‘cyclic’ genes. Expression of cyclic genes occurs in subsequent waves that sweep through the psm once during the formation of each somite (Forsberg et al., 1998; McGrew et al., 1998; Palmeirim et al., 1997). The

segmentation clock is closely linked to Notch and *Wnt*/β-catenin signalling: cycling genes encode various Notch pathway components (Aulehla and Johnson, 1999; Forsberg et al., 1998; Jiang et al., 2000; Jouve et al., 2000; McGrew et al., 1998; Palmeirim et al., 1997), and the negative regulator of the *Wnt* pathway *axin2* (Aulehla et al., 2003). In addition, mutations in some Notch pathway components as well as in *Wnt3a* severely affect the expression of cyclic genes (Aulehla et al., 2003; Bessho et al., 2001; del Barco Barrantes et al., 1999; Jiang et al., 2000; Jouve et al., 2000).

During somite formation specific identities are imposed on somites according to their axial position (Gossler and Hrabé de Angelis, 1998; Hogan et al., 1985; Meinhardt, 1986). Transplantation experiments in chick (Kieny et al., 1972) and mouse (Beddington et al., 1992) embryos have indicated that positional information is established in the psm prior to the formation of epithelial somites. During subsequent somite differentiation, positional specification leads to unique morphologies of vertebrae along the body axis. Mutational analyses have shown that Hox genes are essential for the specification of vertebral identity (Krumlauf, 1994). During development Hox genes are activated sequentially according to their position in the cluster (Duboule, 1994), leading to unique combinations of Hox genes expressed at different axial levels, which is referred to as ‘Hox code’ (Kessel, 1991; Kessel and Gruss, 1991). In the paraxial mesoderm, Hox genes are generally activated in the posterior presomitic mesoderm and remain expressed in somites and their derivatives with distinct

and appropriate expression boundaries. Recent analyses have shown that at least some Hox genes are additionally activated in bursts in the anterior psm, resulting in dynamic stripes that are correlated with the oscillating expression of cyclic genes (Zakany et al., 2001). In *RBPjk* mutant embryos (*Rbpsuh* – Mouse Genome Informatics) expression of cyclic genes is disrupted (del Barco Barrantes et al., 1999) and Hox gene expression is reduced (Zakany et al., 2001). Likewise, loss or reduction of *Wnt3a* affects vertebral identity and expression of some Hox genes (Ikeya and Takada, 2001), suggesting a link between the segmentation clock, coordinated activation of Hox genes, and positional specification. However, thus far alterations of vertebral identities in mice with disrupted Notch signalling have not been reported.

To further study functions of Notch signalling in the paraxial mesoderm we have generated transgenic mice that express in the paraxial mesoderm a truncated version of Delta1 (*Dll1* – Mouse Genome Informatics), *Dll1^{dn}*, which acts as a dominant-negative molecule in *Xenopus* and chick embryos (Chitnis et al., 1995; Henrique et al., 1997). These mice showed reduced Notch activity in the psm, were viable and displayed defects in somites and vertebrae consistent with known roles for Notch signalling in anteroposterior somite patterning. In addition, *Dll1^{dn}* transgenic mice showed with variable expressivity and penetrance alterations of vertebral identities consistent with homeotic transformations. Likewise, hemizygous transgenic *Dll1^{dn}* mice, which carried only one functional copy of the endogenous *Dll1* gene, as well as mice heterozygous for the *Dll1^{lacZ}* null allele showed changes in vertebral identities, suggesting a previously unnoticed haploinsufficiency for *Dll1*. Also, in mice lacking *Lfng* function (Zhang and Gridley, 1998) or expressing *Lfng* constitutively in the presomitic mesoderm (Serth et al., 2003) identities of vertebrae were changed and axial identity was shifted anteriorly, indicating that levels of Notch signalling as well as cyclic activity of *Lfng* is essential for positional specification in the paraxial mesoderm.

Materials and methods

Constructs and generation of transgenic mice

The C-terminal deletion of 141 amino acids in *Dll1* was generated by introduction of three stop codons and an *XbaI* site using PCR primers *Dll1dn#1* (GTACCATGGGCCGTC) and *Dll1dn#2* (GGGTCTAGACTATTATCATTCAGGTGGAGGCTGGTG). The *msd* promoter is a 1494 bp *FokI* fragment fused to the *Dll1* minimal promoter and exon one up to the ATG (Beckers et al., 2000). The *Mesp2* promoter (a 1.2 kb *PvuII/NcoI* fragment 5' of the ATG of the *Mesp2* ORF) was subcloned from a *Mesp2* clone isolated from a genomic λ EMBL3a ES cell library (Schuster-Gossler et al., 1996). Both promoters were cloned in frame to the first ATG of the *Dll1^{dn}* ORF using *NcoI* sites. The *Mesp2* promoter was additionally cloned in frame to the first ATG of *lacZ*. 3' to the coding regions a SV40 polyadenylation signal was included. Integrity of the constructs was verified by sequencing. Transgenic mice were generated by microinjection of linear construct DNA free of vector sequences into pronuclei of (BALB/cx57BL6)F₁ fertilized eggs according to standard procedures. *Dll1^{lacZ}*, *msd::LfngHA3*, and *Lfng^{lacZ}* mice were described previously (Hrabé de Angelis et al., 1997; Serth et al., 2003; Zhang and Gridley, 1998).

Genotyping of mice

PCR typing was performed using genomic DNA isolated from tail

biopsies or yolk sacs, respectively. Used primers: *msd::Dll1^{dn}* and *Mesp2::Dll1^{dn}*; *melta119* (CGGCTCTTCCCTTGTCTAAC) and *Dll1-dn#5* (TCTAGACTATTATCATTCAGGTGG); *Mesp2::lacZ*: *lacZ3* (CAACTTAATCGCCTTGCAGC) and *lacZ4* (CCAGAT-AACTGCCGTCACCTCC); *msd::LfngHA3*: *Lfng-F7* (CCTGTCCAC-TTTTGGTTTGC) and *Lfng-B13* (CAGAGAATGGTCCCTTGATG); *Lfng* wild-type allele: *lfhs1* (GAACAAATATGGGCATTCACTCCA) and *lfgwF13* (GGTCGCTTCTCGCCAGGGCGA); *Lfng^{lacZ}* allele: *lfwF2* (CCAAGGCTAGCAGCCAATTAG) and *lacZB2* (GTGCT-GCAAGGCGATTAAGTT); *Dll1^{lacZ}* allele: *melta38* (ATCCC-TGGGTCCTTTGAAGAAG) and *lacZ1/Dll1ko* (CAAATTCAGAC-GGCAAACG).

Dll1^{dn} transcripts in *msd-Dll1^{dn}* and *Mesp2-Dll1^{dn}* embryos were detected by RT-PCR on total RNA extracted from day 8.5–10.5 embryos using the RNeasy kit (Qiagen). Primers used were *melta119* and *Dll1-dn#5*. HPRT expression was analysed as control using primers HPRT-5' (CACAGGACTAGAACACCTGC) and HPRT-3' (GCTGGTGAAGAGGACCTCT).

In situ hybridisation

In situ hybridisations on sections were performed according to Lescher et al. (Lescher et al., 1998). Whole-mount in situ hybridisations were performed according to Wilkinson (Wilkinson, 1992) with minor modifications using an InsituPro (Intavis AG number 10,000) for automated sample handling. Probes used were: *Cdx1*, *Dll1*, *Lfng*, *Hes5*, *Hes7*, myogenin, *Pax1*, *Pax9*, *Nkx3.2*, *Raldh2*, *Tbx18*, *Uncx4.1*, *Hoxa4*, *Hoxa6*, *Hoxa9*, *Hoxb3*, *Hoxb4*, *Hoxb6*, *Hoxb8*, *Hoxc5*, *Hoxc6*, *Hoxc8*, *Hoxc9*, *Hoxd1*, *Hoxd3*, *Hoxd4* and *Hoxd9*. *Hoxc5* and *Hoxc6* probes were generated from genomic PCR fragments using primers *Hoxc5-1* (ATGACTTTCTCA-CCTTCCTGCCCC), *Hoxc5-2* (TCTCCTTCCCCAACACCTC-TTAC), *Hoxc6-3* (GTCATTTTGTCTGTCTTGGATTGG) and *Hoxc6-4* (TCTGGATACTGGCTTTCTGGTCC). The SV40pA probe was generated from a 250 bp *XbaI/BamHI* subclone from the 3' end of the *msd-Dll1^{dn}* construct.

Skeletal preparations

Alcian blue/alizarin red skeletal staining was performed according to Kessel and Gruss (Kessel and Gruss, 1991). Single vertebrae were dissected after staining of whole skeletons.

Embryo tail halves culture

Culture of 9.5-day embryo tails was performed as described (Serth et al., 2003).

Results

Vertebral malformations and somite defects in mice expressing a truncated *Dll1* in the paraxial mesoderm

To analyse the consequences of reduced Notch signalling in the paraxial mesoderm we generated transgenic mice expressing a C-terminally truncated *Dll1* cDNA, which was shown to act in a dominant-negative manner in *Xenopus* and chick embryos (Chitnis et al., 1995; Henrique et al., 1997). The mouse *Dll1* cDNA was modified analogously such that only 12 amino acids of the intracellular portion adjacent to the transmembrane domain were retained (see Materials and methods). To express the truncated cDNA in the paraxial mesoderm we first used a region of the *Dll1* promoter ('*msd*') linked to the minimal promoter of *Dll1*, which was shown to direct gene expression specifically into the posterior presomitic mesoderm and newly formed somites of transgenic embryos (Beckers et al., 2000; Serth et al., 2003). The 3' UTR and polyadenylation signal was derived from SV40 (Fig. 1A) and served as RNA tag to confirm

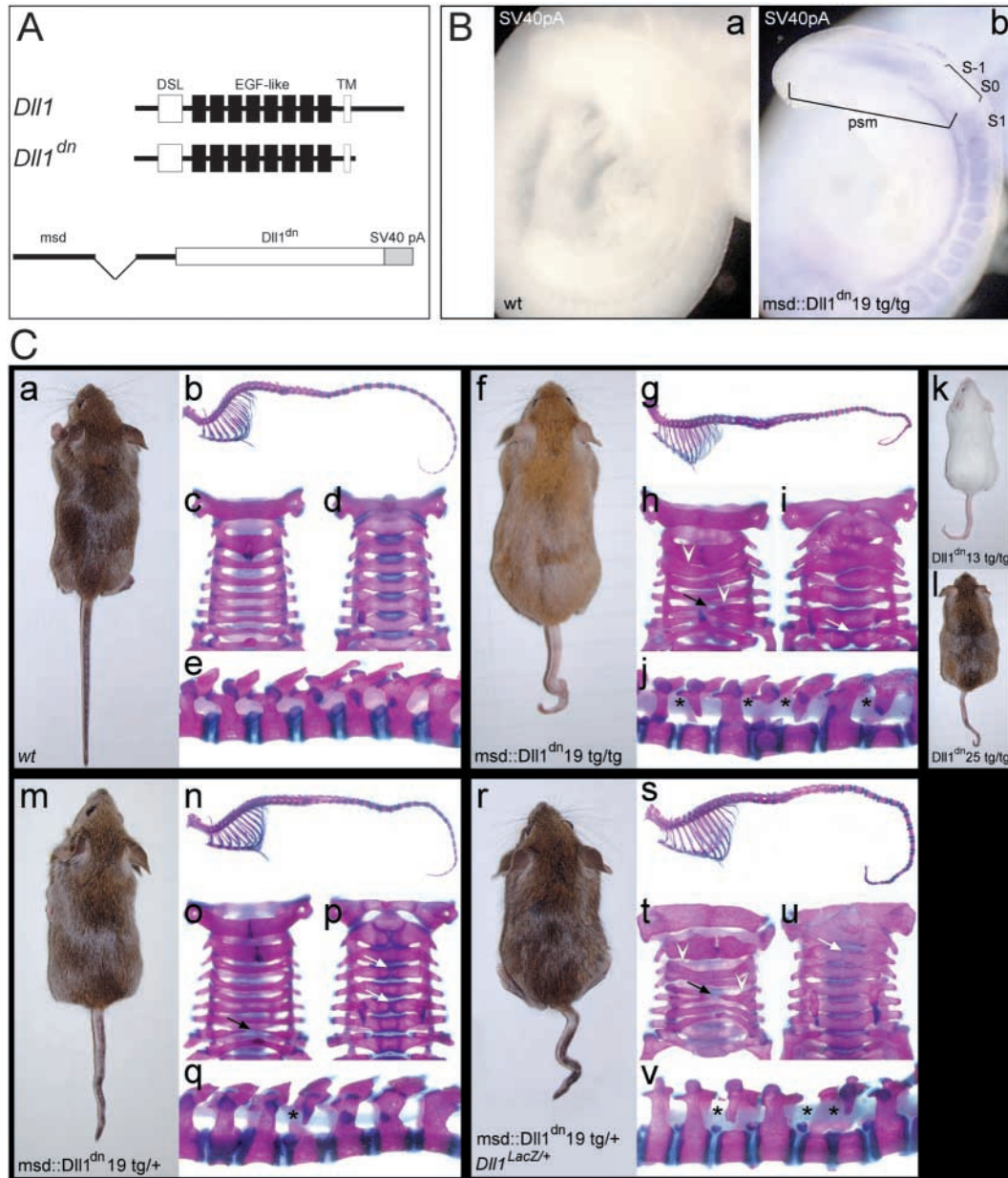
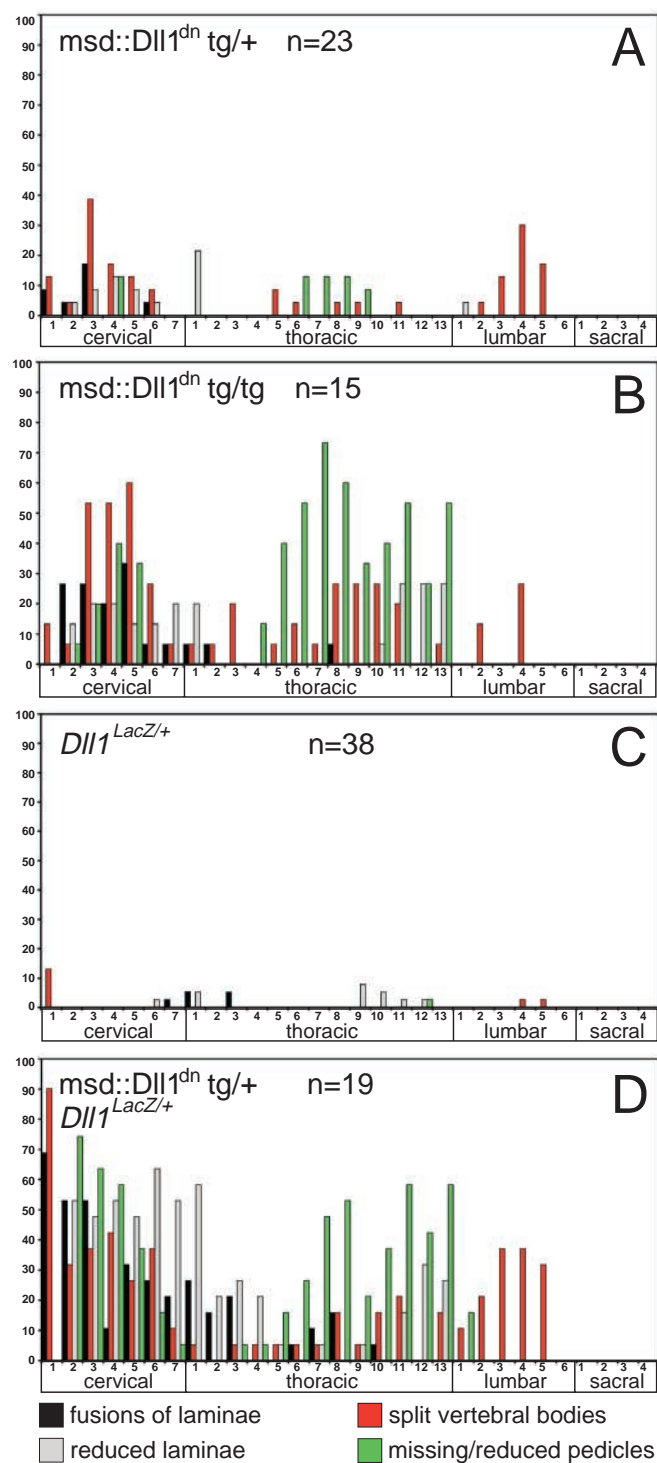


Fig. 1. Transgene expression and phenotypic outcome. (A) Schematic representation of the wild-type and truncated *Dll1* proteins, and structure of the *msd::Dll1^{dn}* transgene. In *Dll1^{dn}* all but 12 amino acids of the intracellular domain proximal to the transmembrane domain have been removed. For details of the construction of *msd::Dll1^{dn}* see Materials and methods. (B) Expression of *msd::Dll1^{dn}* in a homozygous day 9.5 transgenic *msd::Dll1^{dn}* line 19 (b) and wild-type control (a) embryo visualized by whole-mount in situ hybridisation with an antisense probe specific for the SV40pA sequence. Transgene expression is restricted to the posterior psm and recently formed somites. No expression is detected in the anterior psm corresponding to somitomeres S-1 and S0; psm, presomitic mesoderm. (C) External phenotypes and skeletal preparations of 3-week-old wild-type (a-e) and transgenic (f-v) mice. Dorsal (c,h,o,t) and ventral (d,i,p,u) view of the cervical region, lateral view of the whole vertebral column (b,g,n,s) and thoracic region after removal of the ribs (e,j,q,v). Hemizygous transgenic mice (m-q) show kinky tails (m,n), reduced laminae (black arrow in o), split vertebral bodies (white arrows in p) and reduced or missing pedicles (asterisks in q). Expressivity and penetrance of these defects are significantly increased and also fusions of laminae were observed (arrowheads in h,t) in homozygous animals of independent transgenic lines 13, 19 and 25 (f-l) and in hemizygous *msd::Dll1^{dn}* line 19 mice that carry only one functional copy of *Dll1* (r-v).

transgene expression in the paraxial mesoderm of transgenic embryos (Fig. 1B).

Three transgenic founder mice with conspicuous tail defects transmitted the transgene to their offspring, and transgenic lines designated *msd::Dll1^{dn}*13, 19 and 25 were established

(Fig. 1C). Alcian blue/alizarin red-stained skeletal preparations showed that hemizygous mice of all three lines consistently displayed malformations of the vertebral column with incomplete penetrance and variable expressivity. Most prominent were fusions of neural arches predominantly in the



cervical region, reduction or loss of pedicles and laminae in the cervical and thoracic regions, and split vertebral bodies (Fig. 1C, parts o-q, and data not shown).

If the truncated *Dll1* acts also in mouse as a dominant-negative molecule and inhibits Notch signalling, increasing the dose of the transgene, or reducing endogenous Notch activity should enhance the observed defects. Consistent with this idea, external phenotypes and vertebral defects were more severe, and their penetrance was increased in homozygous transgenic

Fig. 2. Distribution and frequency of skeletal malformations. Percentage of observed malformations along the vertebral column in transgenic *msd::Dll1^{dn}19* and mutant *Dll1^{LacZ}* mice. Heterozygous *Dll1^{LacZ}* mice (C) show a low frequency of all four types of malformations analysed. In hemizygous *msd::Dll1^{dn}* mice (A) most prominent phenotypes are split vertebral bodies in the cervical and lumbar region, missing or reduced pedicles mainly found in the central thoracic region as well as fusions or reductions of laminae. Increasing the dose of *Dll1^{dn}* in homozygotes (B) as well as reducing endogenous *Dll1* levels in double heterozygous *msd::Dll1^{dn}/Dll1^{LacZ}* mice (D) increased expressivity and penetrance of all phenotypes. Wild-type control animals (*n*=11) did not show any of the defects observed in transgenic or mutant mice (data not shown). *n*, number of analysed animals.

mice from all three lines (*n*=7, 15 and 15, for *msd::Dll1^{dn}13*, 19 and 25, respectively (Fig. 1C, parts f-l, Fig. 2, and data not shown). Likewise in hemizygous *msd::Dll1^{dn}19* mice that carried only one copy of the *Dll1* WT allele, vertebral defects were enhanced (Fig. 1C, parts r-v, and Fig. 2D). In addition, expression of *Hes5*, which is a transcriptional target of Notch (Ohtsuka et al., 1999; Shimizu et al., 2002) and expressed in the psm of WT embryos in variable stripes (Fig. 3A,B, and data not shown), was not detected in the psm of homozygous *msd::Dll1^{dn}19* embryos between day 9.5 and 11.5 of development, whereas expression in the neural tube was unaffected (Fig. 3C,D, and data not shown). Together, these data indicated that *Dll1^{dn}* indeed acts in a dominant-negative manner and reduced Notch signalling in the psm.

The reduction or loss of pedicles in *msd::Dll1^{dn}* transgenic mice is reminiscent of, although milder than, the phenotype of mice lacking *Uncx4.1* function (Leitges et al., 2000; Mansouri et al., 2000). Because *Uncx4.1* expression is lost in the *Dll1* null mutant (del Barco Barrantes et al., 1999), a reduction of *Uncx4.1* could underlie the pedicle defects. Consistent with this idea, in homozygous transgenic day 9.5 *msd::Dll1^{dn}19*, and hemizygous *msd::Dll1^{dn}19* day 9.5 embryos with only one copy of wild-type *Dll1*, *Uncx4.1* expression in the prospective cervical and thoracic regions was reduced, similar to mouse embryos homozygous for a mutation that prevents efficient proteolytic processing of Notch1 (Huppert et al., 2000), and *Tbx18* expression domains, which delineate anterior somite regions, were expanded (Fig. 3F,H,J,L, and data not shown). *Pax9*, which is normally expressed at high levels in the posterior-lateral sclerotome of each segment, showed less distinct domains of strong expression in posterior somite halves (Fig. 3N,P), whereas expression of other sclerotome markers such as *Nkx3.2* and *Pax1* was not obviously altered in *msd::Dll1^{dn}* embryos (data not shown). This suggested that somite compartmentalisation was affected in *msd::Dll1^{dn}19* transgenic embryos, although distinct anterior and posterior compartments were clearly present. Analysis of myogenin, a marker for myotome, showed occasional subtle alterations of expression domains (see Fig. 8B), but fusions of adjacent myotomes that were found in *Dll1* null embryos were not observed in transgenic day 9.5 and day 10.5 embryos (*n*=5, respectively).

Changes in vertebral identities and subtle alterations of Hox gene expression

In addition to the vertebral malformations described before, the

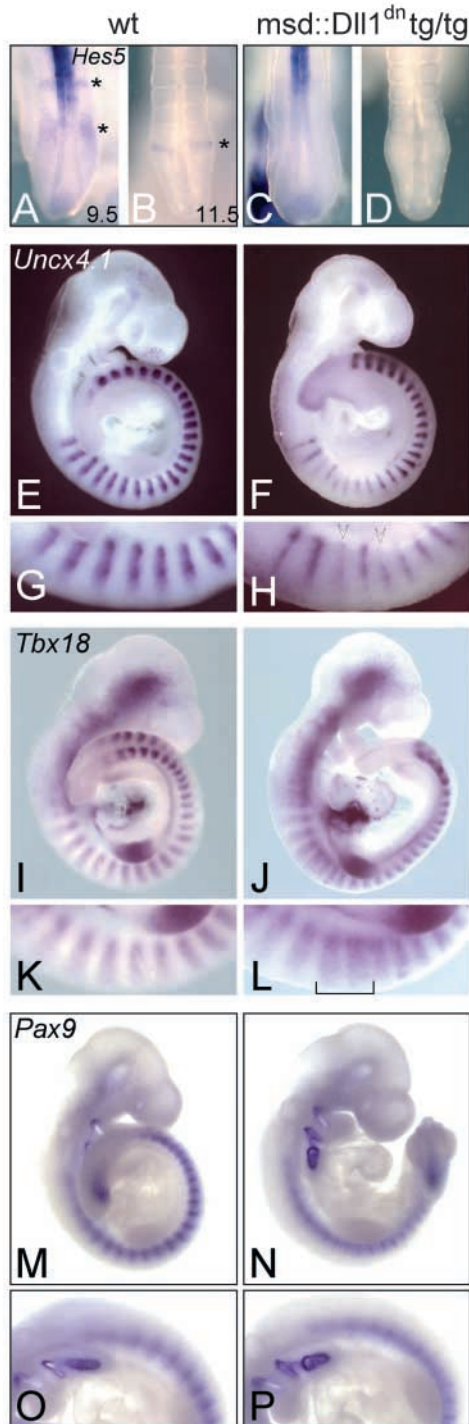


Fig. 3. Reduced Notch activity and AP patterning defects in *msd::Dll1^{dn}* homozygous embryos. Consistent with reduced Notch activity in *msd::Dll1^{dn}* embryos, expression of the Notch target *Hes5* was not detected in the presomitic mesoderm of day 9.5 and 11.5 *msd::Dll1^{dn}* embryos (C,D) in contrast to wild type (asterisks in A,B). *Uncx4.1* expression (E-H) in posterior somite halves was significantly downregulated in transgenic embryos (arrowheads in H), whereas expression of the anterior somite compartment marker *Tbx18* (I-L) was expanded into posterior somite halves (bracket in L) of day 9.5 embryos. Differential expression of the sclerotome marker *Pax9* in anterior and posterior somite compartments (M-P) was less distinct in *msd::Dll1^{dn}* day 9.5 embryos particularly in the cervical region (N,P).

Fig. 4A) but not at C7. In addition, mice with a normal C6 and uni- or bilateral anterior tuberculi on C7 were observed (Table 1). Thus, in hemizygous *msd::Dll1^{dn}*19 transgenic mice C6 resembled at least in part C5, and C7 had acquired properties typical for C6, suggesting that the identities of C6 and C7 were altered. These alterations were enhanced and fully penetrant in animals of all three homozygous *msd::Dll1^{dn}* lines. In 40% of *msd::Dll1^{dn}*19 homozygotes ($n=15$) both ventral processes were missing at C6, and both sides of C7 carried either a ventral process or a transverse foramen (Fig. 4C,C'), whereas the remainder had unilateral transformations. In addition, in two cases the ribs attached to the first thoracic vertebra (T1) were reduced (grey arrowheads in lower-right panel in Fig. 4C), and in one such skeleton eight ribs were unilaterally attached to the sternum (data not shown). Overall, the observed alterations are consistent with anterior homeotic transformations in the cervical and upper thoracic regions. Reduction of endogenous *Dll1* in hemizygous *msd::Dll1^{dn}*19 mice that carried one copy of the *Dll1^{lacZ}* null allele ($n=16$) led to alterations of vertebral identities in 87% of the cases (Fig. 4D,D', Table 1). However, in contrast to hemizygous and homozygous *msd::Dll1^{dn}*19 mice, which exclusively displayed anterior transformations, phenotypes in some compound heterozygotes were more complex. In one case C6 appeared essentially normal, C5 carried small ventral processes that resembled small anterior tuberculi, and C7 had acquired ossified structures that might represent rudimentary ribs or portions thereof (left panels in Fig. 4D, and Table 1). In two other cases C6 had lost its characteristics and resembled C7, whereas C5 and C7 had acquired structures not typical for these vertebrae (right panels in Fig. 4D, and Table 1). Together, the alterations in these mice suggested that they carried composite anterior and posterior transformations. This prompted us to analyse in more detail the vertebral columns of heterozygous *Dll1^{lacZ}* mice ($n=38$). Four of these had rudimentary ribs uni- or bilaterally on C7 (Fig. 4E,E', Table 1, and data not shown), suggesting a previously unnoticed haplo-insufficiency for *Dll1* in the paraxial mesoderm. In contrast to *msd::Dll1^{dn}*19 mice, alterations in the cervical region resembled posterior transformations (Table 1).

The *msd* promoter fragment directed gene expression into the posterior psm and newly formed somites with a gap of expression in the anterior psm corresponding to S-I/S0 (Fig. 1B). To address whether the reduction of Notch signalling in the anterior psm is sufficient to induce alterations of vertebral identities, we generated transgenic mice carrying the truncated *Dll1* cDNA under the control of the *Mesp2* promoter (Fig. 5A).

ventral processes (anterior tuberculi) characteristic for the sixth cervical vertebra (C6) of WT mice (white arrowheads in Fig. 4A) were located abnormally in 74% of hemizygous *msd::Dll1^{dn}*19 mice ($n=23$) (Fig. 4B,B', Table 1, and data not shown). Anterior tuberculi were either unilaterally or bilaterally reduced or missing on C6 (black arrowheads in Fig. 4B), which was accompanied by the unilateral presence at the seventh cervical vertebra (C7) of either a ventral structure or a transverse foramen (white arrowheads or arrow, respectively, in Fig. 4B), which is normally present at C3 to C6 (arrows in

Table 1. Homeotic transformations in the cervical region of *Dll1^{dn}* and *Dll1^{lacZ}* mice

<div> <div>C4</div> <div>C5</div> <div>C6</div> <div>C7</div> <div>T1</div> </div>														
	none	transformation												
		anterior							posterior			bidirectional		
		complete		partial					complete		partial	partial	partial	
		C6-> C5 C7-> C6	C7-> C6	C7-> C6	C6-> C5			T1-> C7	C5->C6 C6->C7	C7-> T1	C7-> T1	C4 <-> C5 <-> C6	C5 <-> C6 <-> C7	
<i>Dll1^{dn}</i> tg/+ n=23	26%													
<i>Dll1^{dn}</i> tg/tg n=15	0%													
<i>Dll1^{dn}tg/+</i> <i>Dll1^{lacZ}+/+</i> n=16	13%													
<i>Dll1^{lacZ}+</i> n=40	87.5%													

Schematic representation and summary of changes in vertebral identities. Seventy-four percent of hemizygous transgenic mice showed complete (26%) or partial (48%) anterior transformations in the cervical column, indicated by the presence/absence of anterior tuberculi, transverse foramina or ribs. In homozygous animals, the penetrance increased to 100% with a higher rate of complete transformations (40%). Double heterozygous *msd::Dll1^{dn}; Dll1^{lacZ}* animals showed anterior transformations (63%) as well as posterior (6%) and bidirectional (18%) transformations. In heterozygous *Dll1^{lacZ}* mutants, only posterior (10%) or bidirectional (2.5%) homeotic transformations were observed with incomplete penetrance.

This directs heterologous gene expression in the anterior psm corresponding approximately to S-I (Haraguchi et al., 2001). Hemizygous transgenic mice of four independent lines carrying this construct were externally indistinguishable from non-transgenic littermates and had no obvious defects in their axial skeletons, although embryos expressed the transgene from day 9.5 onwards at levels readily detected by RT-PCR (lines #4 and #5 in Fig. 5C, and data not shown). Also homozygous *Mesp2::Dll1^{dn}* mice (homozygosity ascertained by test-matings with WT females or males, respectively) generated from line #4 were externally normal, although Notch activity was attenuated in the anterior psm as indicated by reduced *Hes5* expression in homozygous day 9.5 ($n=4$) and 11.5 ($n=2$) *Mesp2::Dll1^{dn}* embryos (Fig. 5D). However, skeletal preparations showed changes in vertebral identities: four out of ten mice had only 5 lumbar vertebrae and 14 pairs of ribs with eight ribs attached to the sternum (Fig. 5E,F), whereas no malformations in the cervical region were found, which might be because of the absence of significant levels of transgene expression prior to day 9.5 (data not shown).

Numerous studies have shown that loss of individual Hox genes, alteration of their expression domains, or disruption of their temporal regulation causes homeotic transformations in mice (e.g. Jeannotte et al., 1993; Kessel et al., 1990; Kessel and Gruss, 1991; Ramirez-Solis et al., 1993; Zakany et al., 1997). To address whether *Dll1^{dn}* activity affects Hox gene

expression, we analysed the expression of various Hox genes in homozygous *msd::Dll1^{dn}* transgenic embryos between embryonic day 8.5 and 12.5. We focused on 15 genes whose published anterior expression borders lie in the regions with observed phenotypic alterations, and on genes that were shown by mutational analyses to be important for the specification of vertebrae, which were transformed in *msd::Dll1^{dn}* mice (for probes see Materials and methods). Whole-mount in situ hybridisation of transgenic day 8.5, 9.5 and 10.5 embryos did not show obvious spatial or temporal alterations of Hox gene expression in the paraxial mesoderm (data not shown). To analyse the spatial distribution of Hox gene transcripts more precisely, in situ hybridisations were performed with *Hoxb3*, *Hoxb6*, *Hoxc5* and *Hoxc6* on sagittal sections of paraffin embedded homozygous transgenic day 12.5 *msd::Dll1^{dn}* and with *Hoxc8* on *Mesp2::Dll1^{dn}* embryos. In WT embryos ($n=5$) *Hoxb6* expression was readily detected in prevertebra seven and subsequent posterior segments (Fig. 6A,A') as described previously (Akasaka et al., 1996). However, in six out of 18 *msd::Dll1^{dn}* embryos *Hoxb6* transcripts were only detected in and posterior to prevertebra eight (Fig. 6B,B'). Likewise *Hoxc5* expression was barely detected in six out of 16 embryos in prevertebra C7 normally expressing the gene at high levels (Fig. 6E,E'), whereas the anterior expression borders of *Hoxb3*, *Hoxc6* and *Hoxc8* were unaltered ($n=8$, 7 and 7, data not shown). In addition, consistent with the low penetrance of

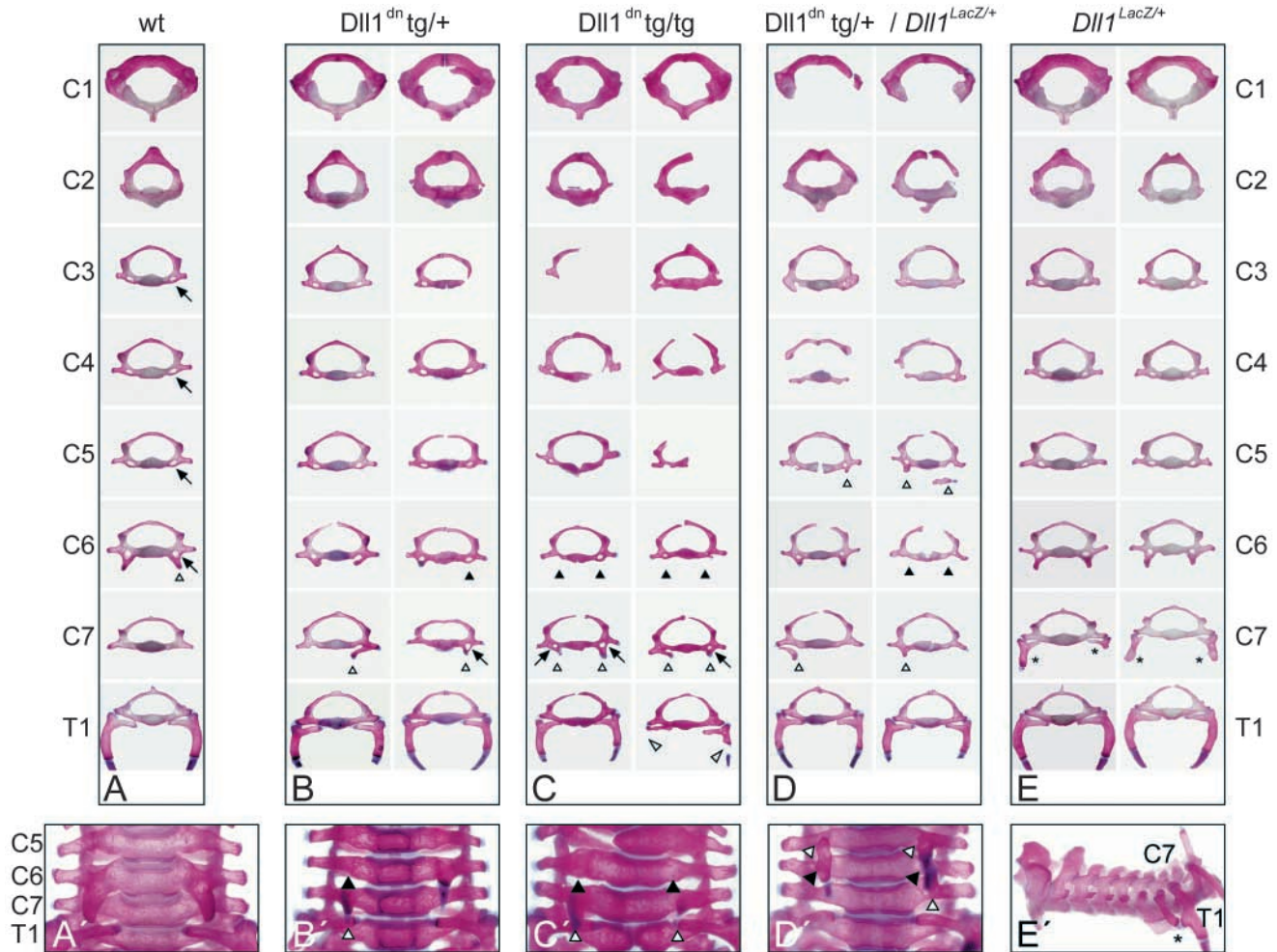


Fig. 4. Homeotic transformations in the cervical vertebral column. Isolated individual vertebrae and cervical vertebral columns after Alcian blue/alizarin red staining. Ventral processes (anterior tuberculi) present at wild-type vertebrae C6 (A,A') were unilaterally or bilaterally missing (black arrowheads) in hemizygous (B,B') and homozygous (C,C') *msd::Dll1^{dn}* and most double heterozygous *msd::Dll1^{dn}; Dll1^{lacZ/+}* (D,D') mice. In hemi- or homozygous animals this was accompanied by the presence of ventral structures (white arrowheads, B,B',C,C') and/or transverse foramina (arrows, B,C) on C7 and reduction of ribs at T1 (grey arrowheads, C). In *msd::Dll1^{dn}; Dll1^{lacZ/+}* mice aberrant ventral processes were found on C5 or C7 (white arrowheads, D,D'). In some heterozygous *Dll1^{lacZ}* mutant mice rudimentary ribs were attached to C7 (asterisks, E,E'). Arrows in (A) point to the foramina at C3-C6.

posterior transformations, in two out of 12 heterozygous day 12.5 *Dll1^{lacZ}* embryos *Hoxb6* transcripts were detected ectopically in prevertebra six (Fig. 6C,C', and data not shown). Interestingly, loss of *Hoxb6* resulted in anterior transformations of C6 through T1 (Rancourt et al., 1995), suggesting that altered *Hoxb6* expression contributes to the transformations in *msd::Dll1^{dn}* and *Dll1^{lacZ}* mice. To address whether the shift of *Hoxb6* expression is evident earlier, we analysed day 8.5, 9.5 and 10.5 *Dll1^{dn}* embryos ($n=15$, 30 and 20, respectively) for *Hoxb6* expression by whole-mount in situ hybridisation. However, no consistent differences to WT embryos were detected. Homeotic transformations in the cervical and upper thoracic region were also found in mice lacking the caudal-type homeobox protein *Cdx1* (Subramanian et al., 1995), and reduced *Cdx1* expression may cause transformations in *Wnt3a* mutants (Ikeya and Takada, 2001) raising the possibility that *Cdx1* expression might be affected in *msd::Dll1^{dn}* embryos. However, no alterations of *Cdx1* expression were found in day 9.5 transgenic embryos (data not shown).

To address whether altered expression of cyclic genes in the psm might underlie altered vertebral identities and altered Hox gene expression in *msd::Dll1^{dn}* embryos, we analysed expression of *Lfng* and *Hes7*, two cyclic genes essential for somite formation and patterning (Bessho et al., 2001; Evrard et al., 1998; Zhang and Gridley, 1998). *Lfng* patterns corresponding to all phases of the expression cycle were observed in transgenic day 9.5 embryos ($n=39$), with a distribution of embryos in the various phases of the expression cycle indistinguishable from WT embryos ($n=40$; data not shown). Embryo halves cultures also indicated cyclic *Lfng* expression in transgenic embryos (data not shown). Likewise, no obvious deviations from normal *Hes7* expression ($n=10$) were observed, and *Hoxd1* expression in the anterior psm was indistinguishable from WT ($n=13$; data not shown). Thus, reduced Notch activity can change vertebral identities and alter Hox gene expression without readily detectable changes in cyclic gene expression in the psm.

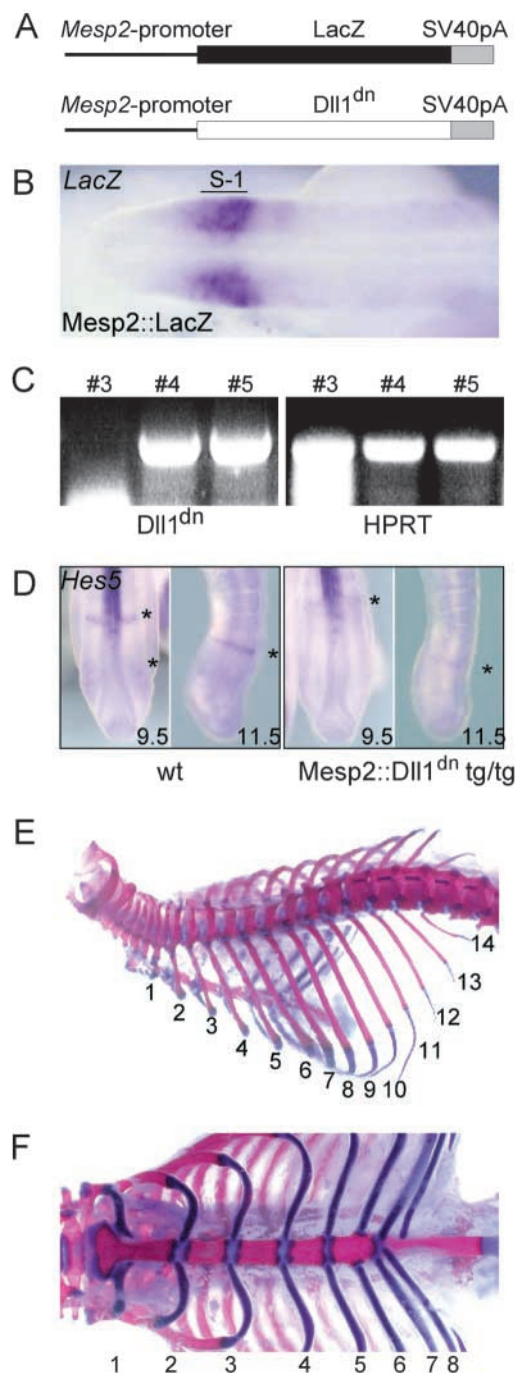


Fig. 5. *Mesp2::Dll1^{dn}* transgene expression and phenotype.

Schematic representation of transgenic constructs (A) directing heterologous gene expression into the anterior region of the psm corresponding approximately to somitomere S-1 as indicated by whole-mount in situ hybridisation of a day 9.5 *Mesp2::lacZ* transgenic embryo (B). Expression of *Dll1^{dn}* detected by RT-PCR in transgenic lines #4 and #5 (C). *Hes5* expression (asterisks) in tailbuds of day 9.5 (dorsal views) and 11.5 (lateral views) wild-type (left) and transgenic embryos (right) (D). Note the reduction of *Hes5* in the psm of transgenic embryos. Skeletal preparation of a homozygous *Mesp2::Dll1^{dn}* line 4 mouse showing 14 ribs (E), with 8 ribs attached to the sternum (F).

Lfng activity is a critical parameter of Notch signalling in the psm. Vertebral malformations in these mice make it difficult to unambiguously assign axial identities to each vertebra. However, the ventral arch of C1, the anterior tuberculi normally present at C6, and the spinous process of T2 could be clearly distinguished and were used as landmarks to analyse this region of the axial skeleton. A consistent feature of all analysed skeletons of *Lfng* null mice ($n=7$) was a reduced number of cervical vertebrae and ribs (Fig. 7C). In five cases, the second vertebra anterior to the first rib-bearing vertebra T1 (C6 in WT mice) had two ventral processes resembling the anterior tuberculi present on WT C6. The remainder had one of these processes shifted to either the next anterior or posterior vertebra. In addition, in four skeletons the number of ribs attached to the sternum was reduced (Fig. 7). Transgenic mice with constitutive *Lfng* expression in the psm ($n=11$) showed similar defects. Five *msd::LfngHA3* mice had only six cervical vertebrae, accompanied in part with additional alterations (Fig. 7). In all transgenic mice the number of ribs was reduced, and in four cases also the number of ribs attached to the sternum was altered (Fig. 7C).

The reduction of cervical vertebrae could reflect fusions of initially seven prospective cervical segments during sclerotome formation and subsequent differentiation, or could indicate an anterior shift of posterior axial identities. To distinguish between these possibilities we analysed the number of segments anterior to the fore limb bud in day 10.5 *Lfng* null or *msd::LfngHA3* transgenic embryos well before formation of vertebral structures using myogenin expression as a marker for the segmentally arranged myotomes. In WT and homozygous *msd::Dll1^{dn}*19 embryos ($n=4$, respectively) myogenin expression indicated seven segments anterior to the fore limb bud (Fig. 8A,B). In contrast, two out of four hemizygous *msd::LfngHA* embryos had only six, and *Lfng* null embryos ($n=5$) had only five myogenin stripes anterior to the fore limb bud, respectively (Fig. 8C,D). Likewise, *Dll1* null embryos ($n=5$), in which *Lfng* expression is severely downregulated, had only five segments preceding the forelimb bud (Fig. 8E). In addition, the number of segments between the fore and hind limb buds was reduced in *Lfng* null and hemizygous *msd::LfngHA3* embryos: whereas 12–13 segments were present in WT ($n=4$) and homozygous *msd::Dll1^{dn}*19 embryos ($n=4$), only nine to 11 segments were found in *Lfng* null ($n=5$) and *msd::LfngHA3* ($n=4$) embryos (data not shown), consistent with the reduced number of thoracic vertebrae indicated by fewer ribs (Fig. 7). Because of fusions between adjacent myotomes in the trunk of homozygous *Dll1^{lacZ}*

Altered vertebral identities in mice with disrupted *Lfng* expression

Because several Hox genes are activated in transcriptional bursts that correlate with dynamic *Lfng* expression (Zakany et al., 2001), we analysed mice lacking *Lfng* function (Zhang and Gridley, 1998), and transgenic *msd::LfngHA3* mice expressing *Lfng* constitutively in the psm (Serth et al., 2003). In embryos of both genotypes *Hes5* expression was either downregulated or not detected ($n=7$, respectively, data not shown), indicating that both loss of *Lfng* function and constitutive *Lfng* activity affect Notch signalling similarly, and supporting that cyclic

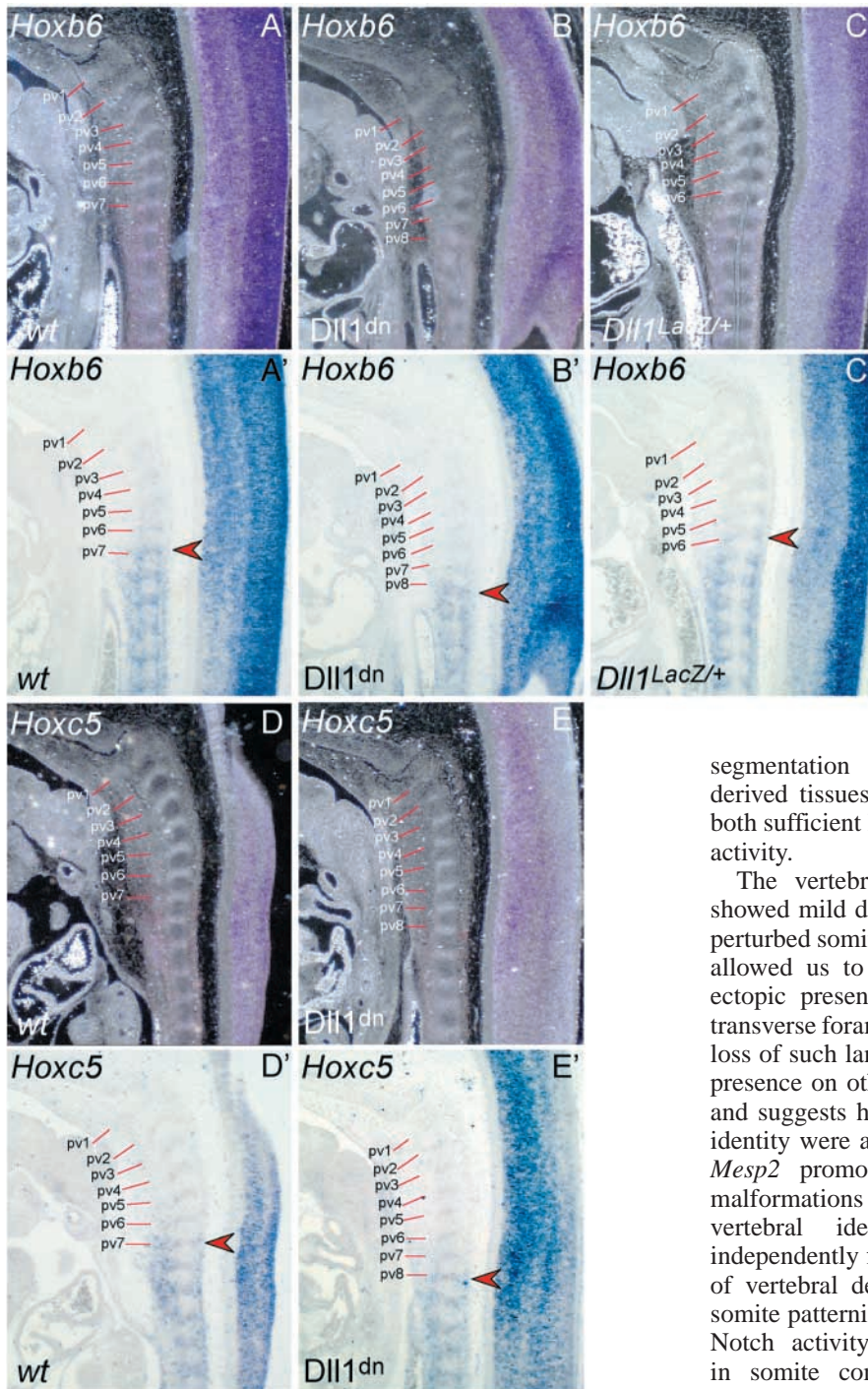


Fig. 6. Alterations in Hox gene expression in *msd::Dll1^{dn}* transgenic mice. In situ hybridisation on sections of paraffin-embedded day 12.5 embryos using Digoxigenin-labeled antisense riboprobes. *Hoxb6* and *Hoxc5* transcripts were detected in prevertebra (pv) 7 and subsequent posterior prevertebrae in wild type (A, A', D, D'), whereas anterior-most expression in transgenic embryos was limited to pv8 (B, B', E, E'). In *Dll1^{lacZ/+}* embryos *Hoxb6* expression was detected in pv6 (C, C'). Arrowheads indicate the anterior-most pv with detected Hox gene expression.

embryos ($n=2$; Fig. 8G, G') in contrast to prevertebra seven in WT embryos (Fig. 8F, F').

Discussion

We have shown that altered Notch signalling in the paraxial mesoderm of mouse embryos changes vertebral identities. Our results provide direct evidence that the coordination of

segmentation and positional specification of mesoderm-derived tissues along the anteroposterior body axis requires both sufficient levels of Notch signalling as well as cyclic *Lfng* activity.

The vertebral columns of *msd::Dll1^{dn}* transgenic mice showed mild defects, which probably reflect consequences of perturbed somite polarity. The largely normal vertebral column allowed us to also unambiguously identify the absence or ectopic presence of landmarks (e.g. anterior tuberculi and transverse foramina) characteristic for particular vertebrae. The loss of such landmarks from some vertebrae and their ectopic presence on others is indicative of altered vertebral identities and suggests homeotic transformations. Changes in vertebral identity were also found in mice expressing *Dll1^{dn}* under the *Mesp2* promoter. In these mice no additional vertebral malformations were detected, suggesting that changes in vertebral identities in *msd::Dll1^{dn}* mice developed independently from segment polarity-related defects. The lack of vertebral defects indicative for disrupted anteroposterior somite patterning in *Mesp2::Dll1^{dn}* mice is surprising because Notch activity in the anterior psm is critically involved in somite compartmentalisation (Takahashi et al., 2003; Takahashi et al., 2000). A potential explanation might be that Notch activity in *Mesp2::Dll1^{dn}* transgenic embryos is higher than in *msd::Dll1^{dn}* embryos, as suggested by residual *Hes5* expression (Fig. 5D), and still sufficient for establishment of segment polarity. The *msd* element directs mRNA expression into the posterior psm and newly formed somites but expression is weak or absent in the anterior region of the psm corresponding to S-I/S0 (Beckers et al., 2000), whereas the *Mesp2* promoter drives expression specifically in this region (Fig. 5B). Thus, in addition to apparently stronger reduction of Notch activity, in *msd::Dll1^{dn}* embryos paraxial mesoderm cells are exposed to reduced Notch activity during most of their progression through the psm, whereas in *Mesp2::Dll1^{dn}*

embryos (Hrabé de Angelis et al., 1997) the number of segments between fore and hind limb buds was difficult to assess unambiguously, but also appeared to be reduced. Together, these results suggested that the reduced number of cervical vertebrae was not because of sclerotome fusions, but the position of the limb buds, and thus axial identity is shifted anteriorly in embryos when cyclic *Lfng* expression and thus probably cyclic Notch activity in the psm is abolished or severely downregulated. Consistent with this idea, the anterior-most expression of *Hoxb6* was detected between prevertebrae four and five in sections of day 12.5 homozygous *Lfng* mutant

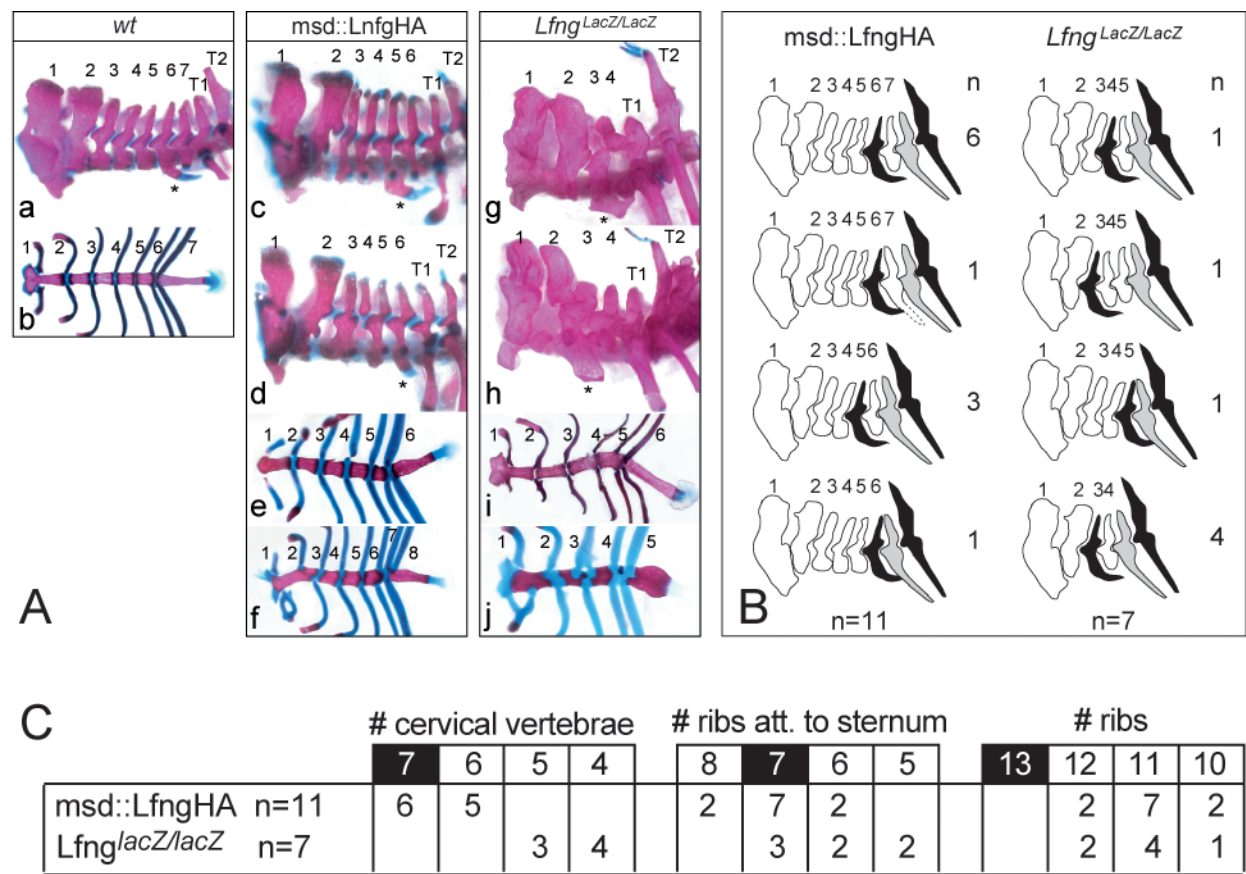


Fig. 7. Transformations in *msd::LfngHA3* and *Lfng^{lacZ/lacZ}* mice. (A) Skeletal preparations of cervical vertebral columns and sterna of transgenic *msd::LfngHA3* and mutant *Lfng^{lacZ/lacZ}* mice. Anterior tuberculi (asterisks) typical for C6 and the anterior-wards directed dorsal spine typical for T2 in the wild type (a) were present in *msd::LfngHA3* (c,d) and *Lfng^{lacZ/lacZ}* (g,h) mice, but the number of cervical vertebrae was frequently reduced in *msd::LfngHA3* and *Lfng^{lacZ/lacZ}* mice. In addition, the number of ribs attached to the sternum (seven in wild type, b) varied from six to eight in *msd::LfngHA3* mice (e,f) and was often reduced to five or six in *Lfng^{lacZ/lacZ}* mice (i,j). (B) Schematic overview of changes in numbers and identities of cervical vertebrae in *msd::LfngHA3* and *Lfng^{lacZ/lacZ}* mice. Vertebrae carrying ventral processes (anterior tuberculi) and dorsal spines used as landmarks are indicated in black, the first rib-bearing vertebra is indicated in grey. In one case rudimentary ribs were found on the seventh cervical vertebra of a *msd::LfngHA3* skeleton. (C) Summary of numbers of cervical vertebrae, ribs, and ribs attached to the sternum in *msd::LfngHA3* transgenic and *Lfng* mutant animals. Normal numbers of skeletal elements in wild-type mice are highlighted.

embryos Notch activity is only reduced in cells shortly prior to somite formation, which might contribute to the phenotypic differences. Formally we cannot exclude that *Dll1^{dn}* expression in the newly formed somites contributed to changes in vertebral identity. However, this seems unlikely because expression in the anterior psm in *Mesp2::Dll1^{dn}* embryos was sufficient to affect vertebral identity. The apparent restriction of changes in vertebral identity to the cervical and upper thoracic region in *msd::Dll1^{dn}* and heterozygous *Dll1^{lacZ}* mice might reflect a higher sensitivity of anterior Hox genes to reduced Notch activity.

The cervical region of transgenic mice expressing *Dll1^{dn}* showed anterior transformations, whereas heterozygous *Dll1^{lacZ}* mice, which presumably have reduced *Dll1*-mediated signals, displayed posterior or bidirectional transformations, and *Dll1^{dn}* mice lacking one copy of *Dll1* had mixed phenotypes. *Dll1^{dn}* rendered chick retina cells deaf to receiving Notch signals (Henrique et al., 1997), blocking Notch activity cell autonomously. Thus, *Dll1^{dn}* appears to not only reduce *Dll1*-mediated Notch signals, but might also affect signals

mediated by other ligands and various receptors, which could lead to different Notch signalling output in the psm than reduction of only *Dll1*. This might not only be a quantitative effect, because in both *Dll1^{dn}* and *Dll1^{dn}/Dll1^{lacZ/+}* embryos *Hes5* expression was severely downregulated and not detected (Fig. 3 and data not shown). Such mode of action of the dominant-negative *Dll1* could explain the different phenotypes in *Dll1^{dn}* and *Dll1^{dn}/Dll1^{lacZ/+}* mice, and would imply that signals mediated by different ligands or receptors contribute to positional specification and might act potentially in opposite ways similar to non-redundant or even counteracting functions during somite compartmentalisation (Takahashi et al., 2003).

Based on the severe reduction of Hox gene expression in day 8.5 *RBPjk* mutant embryos (Zakany et al., 2001), which lack Notch activity, one might expect that attenuated Notch signalling leads to reduced Hox expression. The results of the expression analysis of 15 Hox genes by in situ hybridisation in *Dll1^{dn}* embryos between day 8.5 and 10.5 did not provide evidence for this idea, although we cannot exclude subtle level differences that were not detected by our analysis. However,

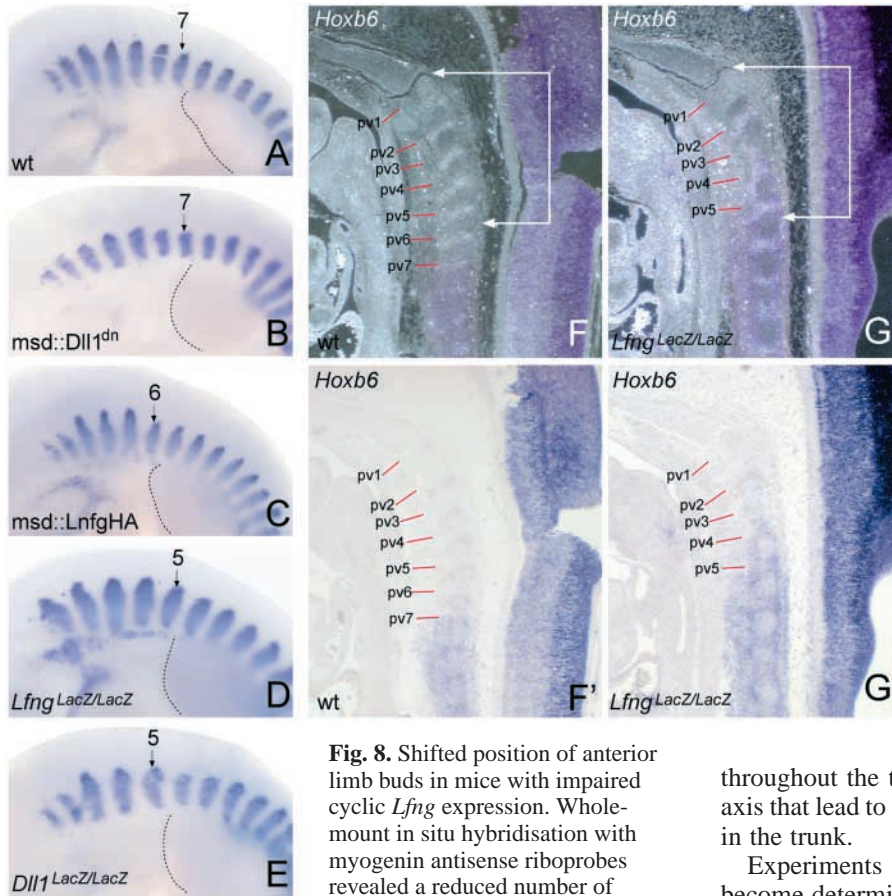


Fig. 8. Shifted position of anterior limb buds in mice with impaired cyclic *Lfng* expression. Whole-mount in situ hybridisation with myogenin antisense riboprobes revealed a reduced number of segmental units anterior to the forelimb bud in *LfngHA3*, *Lfng^{lacZ/lacZ}* and *Dll1^{lacZ/lacZ}* 10.5 day embryos. In wild-type (A) and homozygous *msd::Dll1^{dn}* embryos (B) seven myotomes were detected anterior to the forelimb bud. Transgenic *msd::LfngHA* embryo (C) with six segments anterior to the forelimb bud, and homozygous mutant *Lfng^{lacZ/lacZ}* (D) and *Dll1^{lacZ/lacZ}* (E) embryos with five segments anterior to the forelimb bud, respectively. (G,G') In situ hybridisation on a day 12.5 *Lfng^{lacZ/lacZ}* embryo section showing anterior-most expression of *Hoxb6* between pv4 and pv5 in contrast to pv7 in wild type (F,F'). Brackets in F,G indicate the extent of the first five pv.

forelimb bud in *LfngHA3*, *Lfng^{lacZ/lacZ}* and *Dll1^{lacZ/lacZ}* 10.5 day embryos. In wild-type (A) and homozygous *msd::Dll1^{dn}* embryos (B) seven myotomes were detected anterior to the forelimb bud. Transgenic *msd::LfngHA* embryo (C) with six segments anterior to the forelimb bud, and homozygous mutant *Lfng^{lacZ/lacZ}* (D) and *Dll1^{lacZ/lacZ}* (E) embryos with five segments anterior to the forelimb bud, respectively. (G,G') In situ hybridisation on a day 12.5 *Lfng^{lacZ/lacZ}* embryo section showing anterior-most expression of *Hoxb6* between pv4 and pv5 in contrast to pv7 in wild type (F,F'). Brackets in F,G indicate the extent of the first five pv.

the anterior expression borders of *Hoxb6* and *Hoxc5* were shifted, suggesting that the exact positioning of the rostral limit of Hox expression requires precisely regulated Notch activity in the psm. General Hox activation in the paraxial mesoderm seems to be only affected significantly if Notch signalling is severely reduced or completely blocked potentially already in paraxial mesoderm precursors. How Notch activity and transcriptional regulation of Hox genes are coupled molecularly during paraxial mesoderm formation and patterning requires further investigation.

Transformations of vertebral identities, anterior shifts of *Hoxb6* expression, and of the position of both fore and hind limb buds were detected in mice lacking *Lfng* function or expressing *Lfng* constitutively. An apparent anterior shift of *Hoxb6* expression in *Lfng* mutant embryos could also be expected if fewer segments were generated in the prospective cervical region, whereas the absolute position of the anterior *Hoxb6* expression border along the anteroposterior body axis

was maintained. Recent models of somite segmentation suggest that the interaction of graded FGF (Dubrulle et al., 2001) or WNT (Aulehla et al., 2003) signals with the segmentation clock generates the periodic somite pattern. Conceptually, increasing the steepness of the gradient or slowing the periodicity of the clock would lead to fewer segments, which in either case would be larger. Thus, if the loss of *Lfng* would affect the clock (output) and fewer segments would be formed in the prospective cervical region, they should be larger than normal. However, the five cervical segments in *Lfng* mutant embryos occupied essentially the same space as the anterior five segments in WT embryos (Fig. 8), strongly supporting that the rostral *Hoxb6* expression border is indeed shifted anteriorly. The positions of the fore and hind limb buds are invariant in WT embryos and correspond to the transition between the cervical and thoracic, and lumbar and sacral regions, respectively (Burke, 2000). Their anterior shift suggests homeotic transformations

throughout the trunk region along the anterior posterior body axis that lead to an overall reduction of the number of segments in the trunk.

Experiments in chick embryos indicated that psm cells become determined with respect to the segmentation program and Hox gene expression in the anterior third of the psm at a level referred to as the 'determination front', which appears to represent a threshold level of FGF8 (Dubrulle et al., 2001). Extended exposure of cells to FGF8 in the anterior psm of chick embryos altered the position of somitic boundaries and shifted somitic Hox gene expression boundaries anteriorly (Dubrulle et al., 2001), and hypo- and hypermorphic mutations in FGFR1 caused homeotic transformations and subtle shifts of Hox gene expression borders in mouse embryos (Partanen et al., 1998), indicating that FGF signalling in the anterior psm has a critical role in positioning Hox expression borders. In mouse embryos transcriptional bursts of some Hox genes in the anterior psm correlated with cyclic *Lfng* expression, which has led to the idea that transcriptional regulation of Hox genes just prior to somite formation occurs as a response to the cyclic outcome of Notch activity, which might couple segmentation with the acquisition of axial identity (Zakany et al., 2001). Transformations in vertebral identities along the anteroposterior body axis in mice without *Lfng* function as well as with non-cyclic *Lfng* expression in the psm provide direct experimental evidence that cyclic *Lfng* activity is essential to coordinate the generation of segments with their positional specification. Because the overall specification of different anatomical regions was maintained, colinearity of Hox gene expression was most probably not affected. It has been suggested (Dubrulle et al., 2001; Zakany et al., 2001) that assigning precise combinatorial Hox gene expression to somites occurs in two steps: first, most probably in precursors of the paraxial mesoderm prior to their entering the psm, Hox clusters would be progressively opened and become

transcriptionally accessible. In the second step, in the anterior psm, the definitive expression of Hox genes would be allocated to segmental units coupled to the segmentation clock. Our results are consistent with a critical role of Notch signalling and cyclic *Lfng* activity in the second step, potentially after cells have passed the determination front. Thus, the interplay of FGF and Notch signals in the anterior psm might set definitive rostral Hox boundaries. Posterior transformations were achieved experimentally in transgenic mice by ectopic anterior expression of posterior Hox genes (Kessel et al., 1990; Lufkin et al., 1992; McLain et al., 1992). Likewise, loss of *Lfng* caused posterior transformations and an anterior shift of *Hoxb6* expression. This suggests that *Lfng* activity in the psm is required to prevent ectopic activation, or spreading of Hox gene expression anterior to their normal rostral expression boundaries. Thus, formally cyclic *Lfng* represses Hox gene transcription during setting the definitive anterior expression borders.

Taken together, our data demonstrate that both reduced Notch signalling without detected disruptions of cyclic gene expression in the psm as well as disrupted cyclic *Lfng* activity affect the positional specification of mesodermal derivatives along the anterior-posterior body axis. Thus, Notch signalling and most probably its cyclic modulation are required for the specification of vertebral identities.

We thank Jacqueline Deschamps, Denis Duboule, Mark Featherstone, Peter Gruss, Robb Krumlauf and Tom Lufkin for probes, and Jacqueline Deschamps for critical comments on the manuscript and discussion. This work was supported by the German Research Council (DFG SFB271).

References

- Akasaka, T., Kanno, M., Balling, R., Mieza, M. A., Taniguchi, M. and Koseki, H. (1996). A role for *mel-18*, a Polycomb group-related vertebrate gene, during the anteroposterior specification of the axial skeleton. *Development* **122**, 1513-1522.
- Aulehla, A. and Johnson, R. L. (1999). Dynamic expression of lunatic fringe suggests a link between notch signaling and an autonomous cellular oscillator driving somite segmentation. *Dev. Biol.* **207**, 49-61.
- Aulehla, A., Wehrle, C., Brand-Saberi, B., Kemler, R., Gossler, A., Kanzler, B. and Herrmann, B. G. (2003). *Wnt3a* plays a major role in the segmentation clock controlling somitogenesis. *Dev. Cell* **4**, 395-406.
- Beckers, J., Caron, A., Hrabé de Angelis, M., Hans, S., Campos-Ortega, J. A. and Gossler, A. (2000). Distinct regulatory elements direct *Delta1* expression in the nervous system and paraxial mesoderm of transgenic mice. *Mech. Dev.* **95**, 23-34.
- Beddington, R. S., Puschel, A. W. and Rashbass, P. (1992). Use of chimeras to study gene function in mesodermal tissues during gastrulation and early organogenesis. *Ciba Found. Symp.* **165**, 61-74.
- Bessho, Y., Sakata, R., Komatsu, S., Shiota, K., Yamada, S. and Kageyama, R. (2001). Dynamic expression and essential functions of *Hes7* in somite segmentation. *Genes Dev.* **15**, 2642-2647.
- Burke, A. C. (2000). Hox genes and the global patterning of the somitic mesoderm. In *Somitogenesis*. Vol. 1 (ed. C. Ordahl), pp. 155-183. London, San Diego: Academic Press.
- Chitnis, A., Henrique, D., Lewis, J., Ish-Horowicz, D. and Kintner, C. (1995). Primary neurogenesis in *Xenopus* embryos regulated by a homologue of the *Drosophila* neurogenic gene *Delta*. *Nature* **375**, 761-766.
- Conlon, R. A., Reaume, A. G. and Rossant, J. (1995). *Notch1* is required for the coordinate segmentation of somites. *Development* **121**, 1533-1545.
- del Barco Barrantes, I., Elia, A. J., Wünsch, K., Hrabé De Angelis, M., Mak, T. W., Rossant, R., Conlon, R. A., Gossler, A. and de la Pompa, J.-L. (1999). Interaction between L-fringe and Notch signalling in the regulation of boundary formation and posterior identity in the presomitic mesoderm of the mouse. *Curr. Biol.* **9**, 470-480.
- Duboule, D. (1994). Temporal colinearity and the phylotypic progression: a basis for the stability of a vertebrate Bauplan and the evolution of morphologies through heterochrony. *Development Supplement*, 135-142.
- Dubrulle, J., McGrew, M. J. and Pourquie, O. (2001). FGF signaling controls somite boundary position and regulates segmentation clock control of spatiotemporal Hox gene activation. *Cell* **106**, 219-232.
- Evrard, Y. A., Lun, Y., Aulehla, A., Gan, L. and Johnson, R. L. (1998). *lunatic fringe* is an essential mediator of somite segmentation and patterning. *Nature* **394**, 377-381.
- Forsberg, H., Crozet, F. and Brown, N. A. (1998). Waves of mouse *Lunatic fringe* expression, in four-hour cycles at two-hour intervals, precede somite boundary formation. *Curr. Biol.* **8**, 1027-1030.
- Gossler, A. and Hrabé de Angelis, M. (1998). Somitogenesis. *Curr. Top. Dev. Biol.* **38**, 225-287.
- Gossler, A. and Tam, P. P. L. (2002). Somitogenesis: segmentation of the paraxial mesoderm and the delineation of tissue compartments. In *Mouse Development* (ed. J. Rossant and P. P. L. Tam), pp. 127-153. San Diego: Academic Press.
- Haraguchi, S., Kitajima, S., Takagi, A., Takeda, H., Inoue, T. and Saga, Y. (2001). Transcriptional regulation of *Mesp1* and *Mesp2* genes: differential usage of enhancers during development. *Mech. Dev.* **108**, 59-69.
- Henrique, D., Hirsinger, E., Adam, J., Le Roux, I., Pourquie, O., Ish-Horowicz, D. and Lewis, J. (1997). Maintenance of neuroepithelial progenitor cells by *Delta*-Notch signalling in the embryonic chick retina. *Curr. Biol.* **7**, 661-670.
- Hogan, B., Holland, P. and Schofield, P. (1985). How is the mouse segmented? *Trends Genet.* **1**, 67-74.
- Hrabé de Angelis, M., McIntyre II, J. and Gossler, A. (1997). Maintenance of somite borders in mice requires the *Delta* homologue *Dll1*. *Nature* **386**, 717-721.
- Huppert, S. S., Le, A., Schroeter, E. H., Mumm, J. S., Saxena, M. T., Milner, L. A. and Kopan, R. (2000). Embryonic lethality in mice homozygous for a processing-deficient allele of *Notch1*. *Nature* **405**, 966-970.
- Ikeya, M. and Takada, S. (2001). *Wnt-3a* is required for somite specification along the anteroposterior axis of the mouse embryo and for regulation of *cdx-1* expression. *Mech. Dev.* **103**, 27-33.
- Jeannotte, L., Lemieux, M., Charron, J., Poirier, F. and Robertson, E. J. (1993). Specification of axial identity in the mouse: role of the *Hoxa-5* (*Hox1.3*) gene. *Genes Dev.* **7**, 2085-2096.
- Jiang, Y. J., Aerne, B. L., Smithers, L., Haddon, C., Ish-Horowicz, D. and Lewis, J. (2000). Notch signalling and the synchronization of the somite segmentation clock. *Nature* **408**, 475-479.
- Jouve, C., Palmeirim, I., Henrique, D., Beckers, J., Gossler, A., Ish-Horowicz, D. and Pourquie, O. (2000). Notch signaling is required for cyclic expression of the hairy-like gene *HES1* in the presomitic mesoderm. *Development* **127**, 1421-1429.
- Kessel, M. (1991). Molecular coding of axial positions by *Hox* genes. *Dev. Biol.* **2**, 367-373.
- Kessel, M. and Gruss, P. (1991). Homeotic transformations of murine vertebrae and concomitant alteration of Hox codes induced by retinoic acid. *Cell* **67**, 89-104.
- Kessel, M., Balling, R. and Gruss, P. (1990). Variations of cervical vertebrae after expression of a *Hox-1.1* transgene in mice. *Cell* **61**, 301-308.
- Kieny, M., Mauger, A. and Sengel, P. (1972). Early regionalization of the somite mesoderm as studied by the development of the axial skeleton of the chick embryo. *Dev. Biol.* **28**, 142-161.
- Krumlauf, R. (1994). Hox genes in vertebrate development. *Cell* **78**, 191-201.
- Kusumi, K., Sun, E. S., Kerrebrock, A. W., Bronson, R. T., Chi, D.-C., Bulotsky, M. S., Spencer, J. B., Birren, B. W., Frankel, W. N. and Lander, E. S. (1998). The mouse pudgy mutation disrupts *Delta* homologue *Dll3* and initiation of early somite boundaries. *Nat. Genet.* **19**, 274-278.
- Leitges, M., Neidhardt, L., Haenig, B., Herrmann, B. G. and Kispert, A. (2000). The paired homeobox gene *Uncx4.1* specifies pedicles, transverse processes and proximal ribs of the vertebral column. *Development* **127**, 2259-2267.
- Lescher, B., Haenig, B. and Kispert, A. (1998). sFRP-2 is a target of the *Wnt-4* signaling pathway in the developing metanephric kidney. *Dev. Dyn.* **213**, 440-451.
- Lufkin, T., Mark, M., Hart, C. P., Dolle, P., LeMeur, M. and Chambon, P. (1992). Homeotic transformation of the occipital bones of the skull by ectopic expression of a homeobox gene. *Nature* **359**, 835-841.
- Mansouri, A., Voss, A. K., Thomas, T., Yokota, Y. and Gruss, P. (2000). The mouse homeobox gene *Uncx4.1* acts downstream of Notch and directs the formation of skeletal structures. *Development* **127**, 2251-2258.

- McGrew, M. J., Dale, J. K., Fraboulet, S. and Pourquie, O. (1998). The lunatic Fringe gene is a target of the molecular clock linked to somite segmentation in avian embryos. *Curr. Biol.* **8**, 979-982.
- McLain, K., Schreiner, C., Yager, K. L., Stock, J. L. and Potter, S. S. (1992). Ectopic expression of *Hox-2.3* induces craniofacial and skeletal malformations in transgenic mice. *Mech. Dev.* **39**, 3-16.
- Meinhardt, H. (1986). Models of segmentation. In *Somites in Developing Embryos*. Vol. Life Sciences 118 (ed. R. Bellairs, D. A. Ede and J. W. Lash), pp. 179-189. New York: Plenum Press.
- Ohtsuka, T., Ishibashi, M., Gradwohl, G., Nakanishi, S., Guillemot, F. and Kageyama, R. (1999). *Hes1* and *Hes5* as notch effectors in mammalian neuronal differentiation. *EMBO J.* **18**, 2196-2207.
- Palmeirim, I., Henrique, D., Ish-Horowicz, D. and Pourquie, O. (1997). Avian hairy gene expression identifies a molecular clock linked to vertebrate segmentation and somitogenesis. *Cell* **91**, 639-648.
- Partanen, J., Schwartz, L. and Rossant, J. (1998). Opposite phenotypes of hypomorphic and Y766 phosphorylation site mutations reveal a function for *Fgfr1* in anteroposterior patterning of mouse embryos. *Genes Dev.* **12**, 2332-2344.
- Ramirez-Solis, R., Zheng, H., Whiting, J., Krumlauf, R. and Bradley, A. (1993). *Hoxb-4* (*Hox-2.6*) mutant mice show homeotic transformation of a cervical vertebra and defects in the closure of the sternal rudiments. *Cell* **73**, 279-294.
- Rancourt, D. E., Tsuzuki, T. and Capecchi, M. R. (1995). Genetic interaction between *hoxb-5* and *hoxb-6* is revealed by nonallelic noncomplementation. *Genes Dev.* **9**, 108-122.
- Schuster-Gossler, K., Simon Chazottes, D., Guénet, J.-L., Zachgo, J. and Gossler, A. (1996). *Gtl2^{lacZ}*, an insertional mutation on mouse Chromosome 12 with parental origin-dependent phenotype. *Mamm. Genome* **7**, 20-24.
- Serth, K., Schuster-Gossler, K., Cordes, R. and Gossler, A. (2003). Transcriptional oscillation of *Lfng* is essential for somitogenesis. *Genes Dev.* **17**, 912-925.
- Shimizu, K., Chiba, S., Saito, T., Kumano, K., Hamada, Y. and Hirai, H. (2002). Functional diversity among Notch1, Notch2, and Notch3 receptors. *Biochem. Biophys. Res. Commun.* **291**, 775-779.
- Subramanian, V., Meyer, B. I. and Gruss, P. (1995). Disruption of the murine homeobox gene *Cdx1* affects axial skeletal identities by altering the mesodermal expression domains of Hox genes. *Cell* **83**, 641-653.
- Swiatek, P. J., Lindsell, C. E., Franco Del Amo, F., Weinmaster, G. and Gridley, T. (1994). *Notch1* is essential for postimplantation development in mice. *Genes Dev.* **8**, 707-719.
- Takahashi, Y., Inoue, T., Gossler, A. and Saga, Y. (2003). Feedback loops comprising *Dll1*, *Dll3* and *Mesp2*, and differential involvement of *Psen1* are essential for rostrocaudal patterning of somites. *Development* **130**, 4259-4268.
- Takahashi, Y., Koizumi, K., Takagi, A., Kitajima, S., Inoue, T., Koseki, H. and Saga, Y. (2000). *Mesp2* initiates somite segmentation through the Notch signalling pathway. *Nat. Genet.* **25**, 390-396.
- Wilkinson, D. G. (1992). Whole mount in situ hybridization of vertebrate embryos. In *In Situ Hybridization: A Practical Approach* (ed. D. G. Wilkinson), pp. 75-84. Oxford: Oxford University Press.
- Zakany, J., Gerard, M., Favier, B. and Duboule, D. (1997). Deletion of a *HoxD* enhancer induces transcriptional heterochrony leading to transposition of the sacrum. *EMBO J.* **16**, 4393-4402.
- Zakany, J., Kmita, M., Alarcon, P., de la Pompa, J. L. and Duboule, D. (2001). Localized and transient transcription of Hox genes suggests a link between patterning and the segmentation clock. *Cell* **106**, 207-217.
- Zhang, N. and Gridley, T. (1998). Defects in somite formation in lunatic fringe-deficient mice. *Nature* **394**, 374-377.